Ambient vibration re-testing and operational modal analysis of the Humber Bridge

J.M.W. Brownjohn

Department of Civil & Structural Engineering, University of Sheffield, UK

Filipe Magalhaes, Elsa Caetano, Alvaro Cunha

Faculty of Engineering of the University of Porto, FEUP, Portugal

Contact author: Professor James MW Brownjohn

Department of Civil & Structural Engineering

University of Sheffield

Sir Frederick Mappin Building

Sheffield S1 3JD

E-mail: james.brownjohn@Sheffield.ac.uk

Tel: 0114-2225771

Fax: 0114-2225700

Abstract

An ambient vibration survey of the Humber Bridge was carried out in July 2008 by a combined team from the UK, Portugal and Hong Kong. The exercise had several purposes that included the evaluation of current technology for instrumentation and system identification and the generation of an experimental data set of modal properties to be used for validation and updating of finite element models for scenario simulation and structural health monitoring. The exercise was conducted as part of a project aimed at developing online diagnosis capabilities for three landmark European suspension bridges.

Ten stand-alone triaxial acceleration recorders were deployed at locations along all three spans and in all four pylons during five days of consecutive one-hour recordings. Time series segments from the recorders were merged, and several operational modal analysis techniques were used to analyse these data and assemble modal models representing the global behavior of the bridge in all three dimensions for all components of the structure.

The paper describes the equipment and procedures used for the exercise, compares the operational modal analysis (OMA) technology used for system identification and presents modal parameters for key vibration modes of the complete structure.

Results obtained using three techniques: natural excitation technique/eignsystem realization algorithm, stochastic subspace identification and p-LSCF, are compared among themselves and with those obtained from a 1985 test of the bridge, showing few significant modal parameter changes over 23 years in cases where direct comparison is possible

The measurement system and the much more sophisticated OMA technology used in the present test show clear advantages necessary due to the compressed timescales compared to the earlier exercise. Even so, the parameter estimates exhibit significant variability between different methods and variations of the same method, while also varying in time and having inherent variability.

1 Background

Among all types of civil infrastructure, long span bridges attract the greatest interest for studies of performance by the community of academic researchers and infrastructure operators. Structural Health Monitoring (SHM) applications predominate in bridges and these long term exercises are occasionally linked to short term condition assessment exercises for confirmation of design, as a form of detailed non-destructive evaluation to supplement traditional inspection, for calibration of numerical models, evaluation of simulation strategies, or to provide information for retrofit.

1.1 Long span bridge structural health monitoring (SHM)

For long span bridges (LSBs), SHM is motivated by a range of reasons that typically include effects of unusual or extreme loads such as earthquake, wind or ice sheets, with respective examples of Rion-Antirion, Tsing Ma and Confederation bridges (Le Diourion and Hovhanessian, 2005; Cheung et al., 1997; Wong, 2004). LSB monitoring is commercially viable, with a number of projects installed and operated by monitoring specialists (Andersen and Fustinoni, 2006).

In countries such as Japan (Miyata et al., 2002; Honshu-Shikoku Bridge Authority, 1987) and South Korea (Koh et al., 2009), some form of monitoring of LSBs is mandatory, and it is becoming routine for new LSBs in China and Hong Kong to include comprehensive monitoring, with (at the time of writing) the most complex example in Hong Kong's Stonecutters Bridge (Structural Vibration Solutions, 2009).

When properly managed, such exercises can provide a wealth of information about LSB performance. This is particularly important, since despite new computational capabilities developed within disciplines such as earthquake engineering and aero-elasticity, there are still surprises in real life operational conditions. Bridge engineers still get caught out, usually due to

lack of understanding of loading mechanisms, with famous examples provided by Tacoma Narrows Bridge (University of Washington, 1954) and London Millennium Bridge (Fitzpatrick et al., 2001). Even in recent years, several new LSBs have exhibited unexpected response such as for example due to vortex shedding (Larsen et al., 2000) and excessive stay cable vibrations (Macdonald et al., 2002). It is only possible to mitigate such effects by first observing them and, through monitoring and detailed dynamic investigation, correlate them with loading conditions to arrive at a diagnosis and develop a mitigation strategy.

There are many other motivations for LSB monitoring which for most bridge operators would include assessment of structural condition, confirmation of safe operating conditions and assisting with maintenance decisions. Continuous monitoring aims to address most of these but should be combined with parallel forms of structural investigation, such as periodic visual inspection and more in depth non-destructive evaluation (NDE). One form of NDE that is popular in the research community of SHM is dynamic testing for system identification or modal analysis. Continuous modal analysis is a possibility with a permanent dense sensor array (Pakzad and Fenves, 2009) but a more detailed one-off investigation used to calibrate an optimised sensor array may be a cost-effective solution, and is the strategy being used with a long term monitoring program of the Humber Bridge.

1.2   Dynamic testing for condition assessment and system identification

Dynamic tests of LSBs have a long history. One of the earliest known 'ambient vibration testing' (AVT) exercises, relying on natural wind excitation was a study (Carder, 1937) of the San Francisco-Oakland Bay Bridge and the Golden Gate Bridge in relation to seismic effects. The experimental procedure used a photographic seismograph, and while moving water, traffic, and pedestrian added to the input, the main source of dynamic excitation was wind.

A relatively small number of exercises has used forced vibration testing with large shakers; among these the use of rotating eccentric mass shakers to test the first Bosporus Bridge had

limited success (Tezcan et al., 1975), while much larger shakers have been used by Japanese engineers to test long span bridges such as Ohnaruto and Tatara Bridges (Okauchi et al., 1986). For a few examples (Cunha et al., 2001) free decay to impulsive or suddenly released load has been used.

With very few exceptions, the AVT is now the default procedure for long span bridge dynamic assessment and system identification for recovery of modal parameters. Through the last few decades the technology has been applied e.g. on the Golden Gate Bridge, for the second time, using a specially designed mechanical accelerometer (Vincent, 1962) and the third (but not the last) time, by Nigbor (Nigbor, 1984), who provides the experimental detail behind the results presented later in (Abdel-Ghaffar and Scanlan, 1985), on the Humber Bridge (Brownjohn et al., 1987) at Deer Isle (Kumarasena et al., 1989) , both Bosporus bridges (Brownjohn et al., 1989; Brownjohn et al., 1992), Tsing Ma Bridge (Xu et al., 1997) and Storebælt Bridge, (Frandsen, 2001), to name a few examples. More recent exercises e.g. (Conte et al., 2008; Siringoringo and Fujino, 2006; Brownjohn et al., 2007; Nayeri et al., 2009) have seen the application of operational modal analysis (OMA) techniques capable of resolving true mode shapes, rather than operating deflection shapes (ODS) that are obtained from examination of cross-spectra between response channels, and all these exercises apparently used sensors with conventional cabling arrangements.

1.3   Structural identification

Structural Identification or St-Id is a more detailed exercise than system identification, with the aim of rationalising structural performance to identify and explain load/response mechanisms. Vibration testing by itself only provides modal properties, which typically relate to linear range performance, and all too often data provided by monitoring are merely displayed and stored, or processed in a superficial way. Relatively few examples combine detailed vibration testing with long term monitoring to explain observed performance and hence develop prognosis for future

operation and management.

The WASHMS system for the three bridges of the Lantau Fixed Crossing (Highways Dept, 1993) is one of the better known examples where comprehensive St-Id has had some success. The study of Humber Bridge (Brownjohn et al., 1994) in 1990/1991 by teams from Italy and the UK was an early St-Id example demonstrating the potential for tracking and characterizing operational performance, with the help of the earlier vibration testing exercise.

As well as performance in extreme loads and unacceptable performance during normal loading, LSB operators have concerns about bridge condition such as fatigue damage, seized bearings and deterioration of cables. Some of these concerns are best addressed by conventional inspection and maintenance programs, but the St-Id combination of condition assessment and long term monitoring can provide a wealth of information capable of addressing many of the key concerns.

This is the background to a project funded by EPSRC (Brownjohn and Worden, 2008) to install SHM systems for real-time online structural diagnosis in three major suspension bridges: Humber Bridge and Tamar Bridge in the UK and Fatih Sultan Mehmet (second Bosporus) Bridge in Turkey.

In each case, a combination of static and dynamic instrumentation records loading and performance data to be interpreted by system identification, data mining and computer simulations. The computer simulations using finite element models validated by system identification (modal testing) cover both linear and non-linear response mechanisms likely to cause some of the observed performance effects. This paper describes one part of the project: The system identification exercise for Humber Bridge. The structural identification exercise, including generation of a viable finite element model is a separate study.

2 The Humber Bridge and previous testing

The Humber Bridge (Gurney, 1983) (Figure 1), which was opened in July 1981, has a main span of 1410m with side spans of 280m and 530m. After Severn and Bosporus Bridges, Humber was the third bridge designed by Freeman Fox and Partners having aerodynamic steel box decks and inclined hangers. The spans comprise 124 units of 18.1m long 4.5m deep prefabricated sections 28.5m wide, including two 3m walkways. The top of each box section constitutes an orthotropic plate on which mastic asphalt surfacing is laid, and the sections have four internal bulkheads. At the ends of each span are pairs of A-frame rocker bearings that provide restraint in three degrees of freedom.

The slip-formed reinforced concrete towers rise 155.5 above the caisson foundations and carry the two main cables which sag 115.5m. These cables each have sectional area of $0.29m^2$ and consist of almost 15,000 5mm $1.54kN/mm^2$ UTS wires grouped in strands.

The geometry of the main cable, along with the arrangement of the hangers and bearings are key influences on the dynamic properties of the bridge, as was discovered in previous testing in July 1985 (Brownjohn et al., 1987). The testing was motivated by a requirement to validate finite element (FE) modelling procedures (Dumanoglu and Severn, 1987) for suspensions bridges using the classical SAPIV software (Bathe et al., 1974) developed at University of California, Berkeley. The 1985 testing used only three accelerometers, several km of cables, an analog tape recorder and a two-channel spectrum analyser. By replaying the acceleration signals through the analyser, using a form of the 'peak-picking' procedure to recover frequencies, damping ratios and modulus ratios then laboriously piecing together the mode shape components over a period of six months, it was possible to identify over 100 vibration modes of the main span, side spans and towers up to a frequency of 2Hz. The same FE modelling technology was subsequently applied to the two Turkish suspension bridges (Dumanoglu et al., 1992; Dumanoglu and Severn, 1987) to study the effects of differential support excitation during earthquakes and also validated by full scale testing.

A parallel investigation (in 1985) was carried out by a team from the Building Research Establishment (BRE) (Littler, 1992), who revisited the bridge in 1988. BRE's 1985 test generated six continuous analog recordings of up to 13 hours, while in 1988 a digital tape recorder was left running for eight days, along with an anemometer. The BRE study, which emphasized reliability of modal parameter estimates (particularly damping) was able to show that the modal parameters were not constant but varied with wind speed. In particular the data showed that the frequency of the first lateral mode changed from approximately 0.065Hz in light winds to approximately 0.055Hz in 'strong winds' (possibly from as low as 7m/sec mean wind speed). Observations from the 1985 Bristol measurements and associated FE modeling (Brownjohn et al., 1987) suggested that the pairs of A-frame rocker bearings at each span end, which were designed to prevent translation in vertical and lateral directions, were not functioning correctly. This led to the appearance of the first anti-symmetric vertical vibration mode at a higher frequency than the first symmetric mode, and could have some influence on the functioning of at least the first lateral mode.

In the period 1989 to 1991 a campaign of measurements was organised by University of Bristol in collaboration with Politecnico di Milano in support of performance studies on a design for the proposed Stretto di Messina crossing (Diana et al., 2003). The measurement campaigns (Brownjohn et al., 1994) comprised displacement measurements using optical systems (Zasso et al., 1993; Stephen et al., 1993) and extensive instrumentation with anemometers, extensometers, accelerometers and other forms of novel sensor (Brownjohn, 1990). These measurements were able to identify relationships between wind and temperature loads and static deformations in the form of lateral vertical and rotational movement.

Also, through offline system identification under a wide range of wind conditions it was possible to identify significant aero-elastic influences on vibration modes (Cheli et al., 1992). For example the frequencies of the first vertical and torsional modes were shown respectively to rise and fall, and hence tend to converge, with increasing wind speed. In addition damping ratios

were generally shown to increase significantly with wind speeds. These aero-elastic effects were confirmed in sectional model wind tunnel testing (Curami et al., 1992), but the range of wind speeds during the present test was not sufficient to confirm this behaviour (being below 15m/sec and usually less than 10m/sec).

More recent monitoring exercises on other bridges e.g. (Brownjohn and Carden, 2007) have shown clear influences of temperature on modal parameters, but this was not investigated in the 1985 study. Unfortunately re-processing of the response data is no longer possible because although the data are safely preserved on optical disks, the necessary combination of computer, operating system, interface and driver for reading the data is no longer available.

Deformations of flexible LSBs are of special interest, and for long spans GPS technology is the ideal choice, with successful evaluation for tracking displacements of the tower and deck of the Humber Bridge (Ashkenazi and Roberts, 1997). Other aspects of the bridge performance have also been investigated, for example monitoring of conditions in the anchorage chambers, using wireless sensors (Hoult et al., 2008).

Finally, as part of the EPSRC project (Brownjohn and Worden, 2008) a modest monitoring system including GPS to track main span deformations has recently been installed. This system uses the real time system identification procedures employed at Tamar (Brownjohn and Carden, 2007) to complete, enhance and update the picture of modal parameter variations and their relationship with environmental and structural conditions.

3   Test procedure

The detailed 1985 testing showed that modes existed in which the main span oscillated independently of the side spans, and some modes in which only one side span moved. Because of the signal quality degradation resulting from the analog record/playback process, the modal participation among the spans appeared to be uncertain. Moreover, with only three

accelerometers it was impossible to resolve torsional mode shapes from vertical mode shapes when they occurred at close frequencies. After 23 years the original data are not retrievable and only values in published papers and reports remain. Because of the quality uncertainties and lack of digital data for the EPSRC SHM project, a retest of the bridge was necessary

This was planned to take advantage of new OMA technology, a more comprehensive set of sensors and over two decades of full-scale test experience.

3.1 Modal analysis and instrumentation

The main objective of the test was to identify a set of vibration modes with enough resolution to capture dynamic effects that could be affected by structural changes of interest to the bridge operators and to provide for modal expansion based on the monitored modal response at key positions in the bridge. Going beyond the 1985 results the 2008 testing aimed to identify the contributions of the major bridge components (spans and towers) and relative scales of contributions in the orthogonal axes.

A secondary objective was to provide an extreme test for the range of operational modal analysis (OMA) procedures. The technology of OMA has changed completely since the 1985 testing and a biennial series of 'IOMAC' conferences is presently directed at this technology. With the technology advances, a much more efficient system identification procedure could be applied at Humber.

The instrumentation requirements for very long span bridges are unique: At the time of the test mature, robust and affordable technology for 'real time' synchronous wireless data acquisition from multiple sensors over distances of the order of kilometres was not available to the authors. The 1985 testing used significant cable runs for only two remote sensors but even allowing for multi-signal umbilical cables the logistics of cable procurement and site management would defeat attempts to reduce test time and increase spatial resolution by using a larger number of sensors.

For example the 24-channel vibration testing system used by the first author and members of the Vibration Engineering Section (VES) (Pavic et al., 2008) was designed for 'two-dimensional' structures such as floors and grandstands rather than elongated 'one dimensional' structures such as long span bridges. The limiting capability for this system was exceeded during testing of the Tamar suspension bridge (Brownjohn et al., 2007) ruling out its use at Humber without investment in tens of kilometres of cabling.

Apparently the capabilities of the FEUP (Faculty of Engineering of the University of Porto) research group VIBEST (www.fe.up.pt/vibest) more accurately matched requirements for long span structure testing, as has been demonstrated for a number of long span bridges (Cunha et al., 2001; Cunha et al., 2007). Hence the chosen testing strategy would make use of autonomous recorders with accurate timing of GPS-synchronised clocks and a range of state of the art operational modal analysis (OMA) procedures. The FEUP team provided their set of six GeoSIG recorders, and these were supplemented by a set of four new recorders procured by VES.

While the ten recorders used were almost identical, they used different types of tri-axial sensors. Four recorders used internal Reftek force balance accelerometers, two used external Guralp CMG5 accelerometers and four used external arrangements of Honeywell QA750 servo-accelerometers.

3.2   Test program

With up to five days of measurement available and a maximum of ten hours per day due to recorder battery limitations, an optimal plan was formulated that involved separate recordings (setups) to cover 76 positions along the bridge spans and towers. Sensor locations for one of the setups is shown in Figure 2; in each setup two pairs of tri-axial recorders would be maintained at two permanent reference locations, leaving the remaining three pairs to rove either the deck or the East/West tower pylons. Each measurement setup with ten recorders generated one hour

of 30-channel acceleration records, in four consecutive but not quite contiguous 15-minute segments.

Example auto spectra resulting for the vertical response of one recorder for a single one-hour recording (S7 at location h21) are given in Figure 3, indicating the likely frequency range of interest for modal identification. In fact due to high modal density, time constraints and the greater importance of the lowest modes of vibration, the decision was made to concentrate on the frequency range 0-1Hz.

Each full day of measurements was pre-programmed into each recorder, leaving 10-minute periods between measurements to move the six roving recorders (rovers). Several cross-calibration measurements were made to test the synchronisation and relative calibrations of the recorders by positioning them together. Figure 4 shows the coherence functions and phase angles between four vertical sensors at the same location: the chosen reference among these is sensor S1, and the average drift of 10° between 0Hz and 4Hz corresponds to lag of approximately 7 milliseconds. For modes up to 1Hz the phase angle errors are acceptable.

For side span measurements an extra pair of recorders was kept as a side span reference to allow for the case of completely independent side span modes (leaving four rovers), and on the final day, a single pair of recorders was kept in the main span with a pair of recorders left on the top of each tower (one on each pylon) with the remaining pairs roved in the tower.

There being an average 5km round trip to visit the opposite side of the bridge, teams worked independently on each side of the deck, communicating via cellphone text messages. Bicycles with trailers were used to speed the moving process and with constant pedestrian traffic on the walkways where the recorders were located the recorders had to be guarded constantly. Even during occasional heavy rain, the recorders and sensors worked perfectly.

Measurements on the tower tested the limits of the recorders: the pier movements were expected (from limited measurements in the 1985 testing) to be very small and at the resolution limits of

the sensors, also satellite visibility for the GPS synchronisation was reduced below the deck and was zero inside the towers.

For the 1985 measurements, accelerometers were kept inside the deck to avoid problems with weather. In the 2008 test, an independent recording using a NI-USB 9239 acquisition unit and four QA750 accelerometers was left running inside the deck near the centre span for the duration of the measurements to provide a continuous recording of deck translation and rotation. Local anemometer data were also provided by bridge staff after the testing.

4   System identification procedures

33 measurement setups were completed over the five day period, each with 10 three-axis acceleration measurements and included repeated measurements (at the references). Of these, four measurements were for cross-calibration and two used recorders within towers without GPS satellite visibility. Data were recorded at 76 pairs of deck and tower locations, providing six degrees of freedom (DOF) per pair. Allowing for expected kinematic duplicates, such as pairs of longitudinal and lateral accelerations signals, this reduces to 76×4 independent DOFs. A decision initially to exclude longitudinal motion from the global identification and concentrate on vertical/lateral translations and torsion further reduced this to 76×3=228 DOFs.

To perform modal analysis on all these simultaneously is a significant challenge. Such large channel counts are not usual for civil structural engineering applications, but are common for ground vibration testing of aircraft (Lo et al., 2001) where the advantages of forced vibration arguably allow for more standardised modal analysis procedure.

To manage the large dataset, a range of OMA procedures including the eigensystem realisation algorithm (ERA) (Juang and Pappa, 1985), stochastic subspace identification (SSI) (Van Overschee and De Moor, 1996) and least squares complex frequency domain (p-LSCF) (Magalhaes et al., 2009b) were used to estimate modal properties, with the major challenge

being the merging of data from the 224 degrees of freedom. These techniques were applied to the data at the end of the test, but a relatively simple procedure based on peak-picking technology was used to merge and inspect data sets at the end of each test day to confirm validity of the data and obtain approximate parameter estimates.

The first step for all these procedures was combination of time series data segments from each of the ten separate recorders into single data files for each setup and mapping them to structural DOFs. This step was performed at the end of each day with application of the peak-picking method to the data to provide initial estimates of mode shapes and frequencies.

4.1   ANPSD inspection procedure (peak picking method)

Peak picking is a simple and fast to apply non-parametric method in the frequency domain that is very useful for testing in situ the quality of the collected data. This was performed with data for each day, so that possible failures could be recovered during the following days. This method also allowed the team to obtain reasonable estimates of the most relevant natural frequencies and mode shapes right after the test.

The analysis of the experimental data involved initial pre-processing operations of trend removal, low-pass filtering and re-sampling, considering that the range of frequencies of interest is rather low, of the order of 1Hz, compared to the original sample rate of 100Hz. Resampled time series were saved for analysis using the other techniques (SSI, ERA, p-LSCF).

In order to be able to identify closely spaced modes of different types (vertical bending, lateral bending and torsion) with this simple identification technique, the time series collected in each section were combined to obtain power spectra enhancing each mode type. Therefore, the analysis was focused on the following combined signals: half-sum of vertical accelerations (vertical bending modes), half-difference of vertical accelerations (torsion modes) and average of lateral accelerations (lateral bending modes) collected at the same deck section.

Subsequently, the acceleration time series obtained were divided into several blocks and

average normalized power spectral estimates were obtained. As it was expected that the three deck segments would behave independently for most of the modes, an ANPSD (average normalized power spectrum density function) was calculated for each span. Following the classical peak-picking method, inspection of these spectra allowed easy identification of more than 30 natural frequencies in the frequency range 0-1Hz. The corresponding mode shapes (or strictly speaking operational deflection shapes) were obtained from the transfer functions relating the ambient response at each measurement point with the corresponding response at one of the reference points, effectively the same procedure used (but much less efficiently) for the 1985 analysis.

4.2   NExT/ERA procedure

The NExT/ERA procedure (James III et al., 1995) implemented in the MODAL system identification software (Brownjohn et al., 2001) was used first. The preface NExT refers to the natural excitation technique where impulse response functions generated typically using forced vibration testing are instead created from cross-spectra of ambient vibration response. Hence the first step in the process was creation of cross-power matrices of dimension up to 30×30×900 for each setup from the 2Hz resampled time series, by averaging over the four 15-minute segments, with trend removal but no windowing or overlap. 'DOF' text files were created for each setup to map channels to structural degrees of freedom in the bridge geometry. The whole set of cross-powers was merged into one large matrix with as many columns as reference channels and as many rows as measurement channels. For each setup cross-powers were normalised with respect to the reference channels before merging, with rescaling of the fully merged cross-power matrix by the auto-powers of the chosen reference channels averaged over all the setups.

This is the process of 'gluing' or merging data sets, allowing for extraction of modal properties from the combined spectra, rather than carrying out identification on individual setups and gluing mode shape pieces by normalising to standard phase (0°) and amplitude (unity) at a reference location. The advantage of gluing spectra is that the complete modal solution can be

provided in one go, the disadvantage is computational expense and the possibility of compromise due to variation of modal properties between measurements.

The impulse response functions generated by the inverse Fourier transform of the complete cross-power matrix were used, via Hankel matrices, to identify modes using the eigensystem realisation algorithm (ERA). Possible variables in this procedure include the shape of the Hankel matrices (number of lags used), the number of poles chosen (at least double the maximum number of possible modes) in the identification and the number of reference channels.

Due to limitations of computer memory with MATLAB and the complicated nature of the three-dimensional modes, the procedure was first applied to subsets of e.g. vertical or torsional only data for most reliable results. In these cases, taking only the ten vertical response channels from each setup, cross-power matrices with dimension 5×5×900 were merged, taking advantage of assumed symmetry or asymmetry with respect to the deck centre line (i.e. summing and differencing then slaving nodes).

The nature of the vertical/torsional modes was first identified by analyses with 10×10×900 matrices and no assumption of symmetry. The mix of lateral and torsional response in predominantly lateral or torsional modes was checked by analyses including all four vertical and lateral DOFs at each location i.e. 20×20×900 matrices, then finally analyses were carried out using all 456 DOFs.

The resulting normalised and merged (glued) cross-spectral matrices then featured dimensions of nref (number of reference degrees of freedom) × ndof (total of active degrees of freedom) × 900. The stability of parameter estimates was explored by using different values of nref and ndof (e.g. by excluding first longitudinal then lateral components) and forming rather large Hankel matrices using up to 100 time steps or lags of the 2Hz-sampled impulse response functions, there being little or no improvement with more lags. Extra decimation was also used

17

to enhance ability to identify the lower frequency modes.

4.3   SSI-COV procedure

The collected acceleration time series were also processed with the covariance driven stochastic

subspace identification method (SSI-COV) using MATLAB routines developed at FEUP.

Similar to ERA, this is a parametric algorithm, in time domain, that fits a state space model to

the correlations of the bridge responses driven by ambient excitation (Van Overschee and

De Moor 1996). Theoretically, this method is able to identify closely spaced modes. Therefore,

it should have been possible to process the lateral and vertical acceleration time series together

without any signal pre-combination. However, an initial analysis showed that the large

differences between vibration amplitudes for vertical and lateral directions prevent this joint

analysis, as only the vertical modes appear, the lateral modes being hidden by the noise of

vertical accelerations. Furthermore, the existence of vertical bending and torsion mode shapes

with almost coincident natural frequencies also forced the use of the signal pre-combination.

Without the adopted pre-combination, the method identifies two modes with almost identical

natural frequencies of 0.31Hz, but there is imperfect separation between the vertical bending

and torsion movements. As a consequence, the SSI-COV method was applied to three pre-

combined signals: half-sum of vertical accelerations (for the identification of vertical bending

modes), half-difference of vertical accelerations (for the identification of torsion modes), and

average of lateral accelerations (for the identification of lateral bending modes) collected at the

same deck section.

Usually, SSI-COV is applied to each setup dataset and then the resulting sets of modal

parameters are associated, averaging the natural frequencies and the modal damping ratios

identified in each setup and gluing the mode shapes segments by means of the common

reference sensors. In the present application, this procedure would involve the manual

interpretation of three stabilization diagrams (one for each pre-combined signal) for each setup,

which would give a total of 29x3= 87 stabilization diagrams to be analysed. Hence, an

alternative approach was necessary.

This work follows an approach in which the output correlation matrices obtained from the different setups are stacked on top of each other and the modal parameters are extracted from the resulting correlation matrix, yielding global values for the eigenfrequencies and modal damping ratios. The identified mode shapes appear with the modal components associated with each setup stacked in a global mode shape. It is then necessary to re-scale the partial mode shapes using the common reference modal components. Compared to the NExT/ERA methodology, which scales the data in the frequency domain before the identification, with this approach the scaling is done in the modal components after the identification.

After some trials using 5Hz sampled time series, it was concluded that good results could be obtained using correlations with 199 points (number of blocks of the Toeplitz matrix $j_b = 100$), which contain 199/5x0.056 = 2.23 cycles of the mode with the lowest natural frequency. In order to reduce the calculation effort and the computer memory requirements, only two outputs were selected for reference, these coincide with the test reference sections of the main deck. Thus, the correlation matrices of each setup present five lines (number of instrumented sections) and two columns (number of output elected for reference). As a result, the global correlation matrix is 130×2 and the Toeplitz matrix to which the SVD is applied is 13000×200.

In order to avoid the subjective task of manually selecting one stable pole for each mode, an automatic procedure was used to interpret the stabilization diagrams provided by the SSI-COV method. This method (Magalhaes et al., 2009a) is based on the application of a hierarchical clustering algorithm, which groups the mode estimates presented at the stabilization diagrams with similar natural frequencies and mode shapes. The groups associated with physical modes are the ones that clearly stand out due to their larger number of elements, and the final estimates are then obtained by averaging the estimates inside the selected groups, after the elimination of possible outliers.

4.4   p-LSCF procedure

With the goal of increasing the confidence on the estimated modal parameters the collected data base was also processed with the p-LSCF method, a parametric frequency domain output-only identification algorithm that is described with detail in (Peeters et al., 2004) and also known under its commercial name PolyMAX. In the present work, the slightly different implementation described in (Magalhaes et al., 2009b) was used.

The application of the p-LSCF method also followed a global estimation methodology and was also based on the separated processing of the same three pre-combined signals that were adopted in the application of the SSI-COV method. The analysis was only concentrated on the global modes of the main span of the deck. In this case, global half-spectrum matrices were constructed from the half-spectra matrices associated with each setup. As two references were adopted these are 5×2 matrices. The elements of these matrices were estimated from the inverse Fourier transform of the positive time lags of correlation functions with a maximum time lag of 256 points, after the application of an exponential window with a factor of 0.1 (the amplitude of the last element of the correlation function is reduced 10%). Complementary analyses using longer correlation functions and a higher number of references outputs demonstrated that the increase of the calculation effort is not compensated by an improvement on the quality of the results.

4.5   Variation of modal and environmental parameters/ SSI procedure

Data from the four-channel recorder kept inside the deck were also used to track variability of modal parameters and response levels throughout the measurements, using SSI-COV procedures developed and implemented successfully on Tamar Bridge (Brownjohn and Carden, 2007). Effectively this is a 'blind' automated procedure which, with only four sensor channels, provides no information about mode shapes (which can be retrieved from the other analyses).

5   Results

5.1   Auto spectra

The auto spectra of Figure 3 for the range 0-25Hz represent the response at location h21 which means the Hessle half of the main span at the 10th hanger location away from the exact midspan. The concentration of energy that appears noise-like in the first 5Hz of the vertical response is remarkable.

Zooming in on the first 1Hz with logarithmic axes and SI units (the recorders are essentially seismometers and report in units of gravity or g), Figure 5 shows longitudinal, lateral, vertical and torsional accelerations. The vertical response is the half sum and the torsional response is the difference divided by chord. The 1st torsional mode at around 0.31Hz appears to occur within a few milli-Hz of a vertical mode, and (as previously mentioned) this has consequences on the ability to discriminate the two modes. Also the 'blip' at about 0.05Hz in the lateral response is in fact the first lateral mode, and what at first appears to be typical accelerometer low frequency noise is in fact due to the deck quasi-static rotation due mainly to vehicle loads.

Figure 6 shows the cause of this quasi-static effect via low-pass filtering of the lateral acceleration signals: deck rotation by an angle ϕ is realised as a component of gravity g·sin ϕ projected on the sensing axis of the lateral accelerometers. This component is the same both sides of the deck, separated by distance r=22m, hence the figure presents relative vertical displacement across the deck obtained from each of the ten transducers (five duplicate pairs) via r·ϕ.

Clearly the low frequency response was caused by a heavy vehicle moving across the bridge from Hessle to Barton.

For the longitudinal response, many of the lower frequency modes appear to have significant longitudinal components apparently at levels greater than could be attributed to imperfect levelling of the accelerometers and deck camber.

5.2   Estimates of mode frequency, shape and damping ratio

All the techniques previously described were used to provide mode shape and frequency estimates, and due to the large number of modes generated, only examples identified up to 1Hz are presented. In the various plots, the presented values of frequency and damping are the direct outputs of the estimation techniques. Variation among the frequency values serves to illustrate the uncertainty and likely errors, while the lack of smoothing of mode shapes highlights any anomalies.

Damping estimates were obtained from all methods except ANPSD and are presented here in order to highlight the problems faced when attempting to obtain 'reliable and representative' damping estimates.

5.2.1   Peak-Picking method

Figure 7 shows the ANPSD of the three combined signals for the three spans and also ANPSD of the acceleration time series collected at the towers. The presented plots prove the independent behaviour of the three spans by the existence of independent peaks for each span (only few peaks are common to the three spans), as was anticipated considering the type of connections between the deck segments and the towers. Observation of the spectra also shows a high density of modes in the frequency range 0-1Hz and the existence of groups of closely spaced modes, as for instance around 0.31 Hz, where there are three vertical bending modes (peaks in the spectra of the half-sum of the deck vertical accelerations) and a torsion mode (peak in the spectra of the half-difference of the deck vertical accelerations). The identification of a resonant frequency of 0.056Hz (a period of 18 seconds) in the spectra associated with the lateral direction proves that the accelerometers used are sensitive to such low frequency vibrations. As expected, the spectra of the tower longitudinal accelerations present some peaks which are also associated with vertical bending modes and evidently, some of the lateral modes are also observable on the spectra of the lateral accelerations measured at the towers. However, the levels of vibration observed at the towers are much lower than the ones recorded at the deck level (the amplitude of

the longitudinal accelerations at the top of the towers is about 1/10 of the amplitude of the deck vertical accelerations), which explains the inferior quality of the spectra. Figure 8 shows the lowest five vertical modes. While being a relatively crude method, it is remarkably effective at producing quick and apparently reliable estimates of the natural frequencies and mode shapes.

Due to the context of its application, no attempt was made to provide damping estimates using this method.

5.2.2   NExT/ERA

Figure 9 shows a selection of modes identified by MODAL using NExT/ERA from measurements only in the vertical plane. Tower motion is included only where it is significant, since for some modes inclusion of tower DOFs (and the resulting limitation to only two references in the deck) led to inferior identification. Among these modes, the fundamental vertical mode demonstrates the largest tower motion, which connects main span and side span motion. Mode shapes are unsmoothed, and the cause of the kink in mode 3 is uncertain.

Using ERA the shapes of the two modes reported around 0.31Hz are not perfectly resolved, but are nevertheless distinctive, one being the first torsional mode. Analysis of the half-sum and difference of time series shows clearly that there are two distinct modes, but at frequencies separated by only a few milli-Hz.

Figure 10 shows a set of modes identified from lateral plane measurements. These include the curious lateral component of the torsional mode at 0.309Hz as well as some interesting (if rather bumpy) modes that exist only in the lateral plane. Among these, many involve lateral motion of the towers, here shown only crudely using the tower tip DOFs.

For both lateral and vertical modes, identification performance varied according to variation in parameters for the ERA process e.g. number of poles, lags, references, resampling frequency etc.. Figure 11 shows the tool used to judge the performance for different number of lags for a

fixed number of poles (40): Stable frequency lines (left plot) indicate a reliable frequency estimate while reliable damping is indicated by stable estimates with high EMAC values (Pappa and Elliott, 1993) (right plot). Having similarly chosen an optimum number of poles, visual inspection of similar plots for different combinations of references and resampling rates is used to judge the best aggregate combination of parameters.

Where it is significant, tower participation in these modes is shown crudely in Figure 9 and Figure 10 without any enhancement. In the vertical/longitudinal plane, tower contribution is significant in modes 1, 3 and 4, although in mode 1 it is only the Barton tower that moves. For higher modes, it is mainly the torsional modes that engage the towers (in torsion) although there is small but clear participation of deck and towers in two side span modes (not presented here).

In the lateral direction, as shown in Figure 10, tower participation is more significant, but this has to be viewed in the context of deck lateral response that is around an order of magnitude weaker than in the vertical plane.

More details of the performance of the towers by themselves was obtained in the 1985 study in which using the wired accelerometers, but those measurements were unable to judge the deck/tower coupling to the degree possible using the synchronised autonomous recorders.

One benefit of using multiple degrees of freedom in the recordings is the ability to identify the full three-dimensional character of mode shapes. Analysis of lateral and vertical components for realising torsional modes is presented in Figure 12, using the same scale in the two views, and for simplicity using the kinematic simplification of lateral averages and vertical differences.

Certain modes did not register strongly in all analysis variants, such as the second and third vertical modes and the second lateral mode. All these modes, when identified, showed relatively high damping ratios consistent with low response levels. These are also the modes whose parameters were shown to vary most throughout the test. The lateral mode identified in the 1985 University of Bristol test at 0.456Hz also proved problematic, appearing variously at around

0.428Hz and 0.464Hz, in each case with low EMAC values.

The longitudinal motion of the three spans together was also investigated. Figure 5 shows a strong and broad peak below 0.04Hz and peaks corresponding to modes around 0.12Hz, 0.17Hz, 0.22Hz, 0.31Hz, 0.38Hz and 0.61Hz. Among these the most 'stable' modes i.e. that are identified for a range of analysis conditions are the modes around 0.12Hz and 0.17Hz, as well as at 0.615Hz. This mode, visualised in Figure 13 by transforming the longitudinal motion to vertical motion, appears not to correspond to motion in any other direction, but is consistent with a mode at 0.57Hz predicted by finite element analysis (Dumanoglu and Severn, 1985) and that has predominant longitudinal character.

The full three dimensional analysis using all available degrees of freedom and a more powerful computer confirmed the results obtained using the subsets of DOFs, however it was easier to explore variations on identification using the simplified analyses.

The 'best' parameter identifications among all the variants of ERA are summarised in Table 1 and Table 2.

5.2.3   SSI-COV

In the application of the SSI-COV method state-pace models of orders varying from 20 to 100 were adopted. Figure 14 presents the stabilization diagram obtained for each group of pre-combined signals.

For the half-sum of the vertical accelerations, in the analysed frequency band there are 14 alignments of stable poles. As only the reference sections of the main span were considered, the local mode shapes of the side spans are not correctly identified with this analysis. A supplementary study, just focused on the side spans, was performed for the identification of these local modes. Taking profit from the additional references, it was possible to identify five further vertical bending modes in the frequency range under study.

Concerning the stabilization diagram obtained after the processing of the semi-difference of the vertical acceleration, five clear alignments of stable poles correspond to five torsion modes. One of these is a local mode of the Barton side span with frequency 0.592Hz, the other four are characterized in Figure 15. In the stabilization diagram associated with the lateral accelerations several vertical alignments of stable poles can also be easily identified. In particular, the one associated with the first lateral mode with a natural frequency of 0.056Hz is evident.

The natural frequencies and mode shapes identified with this method are summarised in Table 1 and Table 2. The lateral and the vertical bending modes are very similar to the ones identified with the ERA method and therefore are not presented.

5.2.4   p-LSCF

The processing of the three global half-spectrum matrices (one for each set of pre-combined signals) lead to the stabilization diagrams presented in Figure 16, which contain the estimates delivered by models with orders between 10 and 50. These were automatically analysed with the same algorithm that was used together with the SSI-COV method. The stabilization diagram associated with the half-sum of the vertical accelerations presents 12 very clear alignments. These are associated with 12 vertical bending modes that are characterized in Table 1 by their natural frequency and modal damping ratios. The comparison with the results delivered by the SSI-COV and ERA methods shows that the mode with frequency around 0.172 Hz is missing. Several alternative analyses with different parameters were tested to try to identify this mode but none of them was successful. Regarding the remaining vertical bending modes, the estimates provided by the three methods present almost coincident mode shapes, similar natural frequencies and quite consistent modal damping ratios.

With respect to the processing of the lateral accelerations, surprisingly, the stabilization diagram of the p-LSCF method shown in Figure 16 is quite different from the one delivered by the SSI-COV method. There are far fewer alignments of stable poles and even the presented diagram

was only possible after the application of a high pass filter with a cutoff frequency of 0.05Hz that reduces the influence of the quasi-static component (very relevant in the lateral direction, as illustrated with the spectra presented in Figure 7). Still, it was possible to identify the most relevant lateral bending modes. The results of the p-LSCF method for the lateral modes are compared with those from the other two methods in Table 2. The natural frequencies are similar but considerable differences are observed on the modal damping ratios. All the mode shapes are analogous.

Finally, the processing of the half-difference of the vertical acceleration time series with the p-LSCF method provided the very clear stabilization diagram represented in Figure 16. From this diagram, it was possible to obtain the modal parameters presented in Table 1. A very good correlation is observed between all the characteristics of the torsion modes estimated by the three applied methods.

5.2.5   SSI applied to continuous recording

Figure 17 and Figure 18 present mode frequencies identified by analysing successive one-hour periods of response from the continuous in-deck recording using the automated SSI-COV procedure. For the vertical response, not all known modes are consistently identified and the weaker modes in the range 0.13Hz to 0.23Hz show significant variation which appears not to have random character. The two lowest lateral modes show a distinct daily trend, also seen on other LSBs e.g. Tamar Bridge (Brownjohn and Carden, 2007).

Different combinations of estimation settings were used, including shorter time series duration, with the optimal values for clearest estimation being 130 points in the covariance function at a sample rate of just below 1Hz and maximum order of 40 poles. For the lateral modes, the automated procedure 'identifies' multiple modes below 0.05Hz that are practically certain not to be real structural modes, hence are not shown.

27

Figure 19 is the spectrogram of the vertical and lateral response throughout the testing; this is a moving window short-time discrete Fourier transform with the strength of the frequency component reflected in the lightness of the shading. There is clear correspondence with the identification results of Figure 17 and Figure 18 in several ways.

First, the estimation process is more likely to fail during weak response. Second the stronger bands, reflecting the modes, shows some variation in the same times as for the frequency identification for particular modes. Third, the frequency reduction occurs during the stronger response.

An additional piece of information is the broadness of the 'modal bands' during the stronger response which can be interpreted many ways including higher damping and a greater range of response levels reflected in greater frequency variation. Either way, this shows the challenge for reliable identification.

The analysis was repeated for shorter (20 minute) and longer (2 hour) periods to generate the covariance functions, also using 130 points (lags) in the SSI-COV procedure, with aim identifying the optimal period length for reliable estimates.

Table 3 shows the mean and standard deviation of resulting estimates over all the period in four days of data for three vertical modes and four lateral modes, these being the only modes whose frequency estimates practically do not overlap with nearby modes. Based on experience in the 1980s testing exercises it might have been expected that longer periods would lead to lower and less variable damping estimates, but from this exercise in general the reverse is observed. The standard deviation of the frequency values does not improve much with longer periods hence it might be supposed that the 20 minute would be optimal for long term continuous estimation.

6 Discussion: Performance of identification techniques

The data set consists of signals from 456 degrees of freedom (DOFs) with duplications and

variation of modal parameters and response levels among data groups over the five days of testing. This provides probably the most challenging dataset from field conditions for testing the present state of the art OMA procedures.

As well as providing a rich dataset for finite element model validation and operational performance assessment, the exercise aimed at evaluating the performance of a range of state of the art operational modal analysis techniques. Not only has the exercise served to demonstrate the capabilities and limitations of the techniques and the dependence on the experimental approach, it also points to the best approach for continuous parameter identification in long term monitoring.

6.1   Comparison among OMA techniques

Table 1 compares identification of vertical modes between the various OMA identifications by University of Sheffield (UoS) and FEUP teams using NExT/ERA, SSI-COV and p-LSCF.

Modes up to 1Hz are examined and classified according to symmetry and side span involvement. In fact because the bridge is not symmetric in the side spans, modes that engage side spans do not have simple symmetry so A/S mean having odd/even numbers of nodal points between the towers. Even this system breaks down for the first and fourth vertical modes: the first mode is effectively the first symmetric mode.

Table 2 shows lateral modes identified in the 2008 exercise using NExT/ERA, SSI-COV and p-LSCF. Clear identification of lateral modes is more problematic than for vertical modes. Nevertheless, because of the high damping ratios and significant frequency variation exhibited by these modes, special attention is paid to their significance in the structural performance.

The long term monitoring exercise (Brownjohn et al., 1994) showed modal frequencies to be affected by wind speed in the second, third and fourth significant figures for the first lateral, torsional and vertical modes respectively. Wind speeds (briefly up to 12m/sec) during the 2008 exercise did not vary significantly compared to the longer exercise where wind speeds reached

30m/sec for long enough periods to allow modal parameter identification using 'peak-picking' methods. Hence no attempt has been made here to study wind effects; this is an aspect for more rigorous study in long term monitoring.

There are no systematic differences between frequency values (where obtained) for all three techniques. Among the three techniques, SSI-COV appears to perform best by identifying all modes (with one possible exception). Next best is NExT/ERA, although resulting damping estimates are the highest among the techniques.

For the lateral direction, where response levels are on average an order of magnitude weaker than vertical response (Figure 5) modal identification is less successful and provides the most severe test of the procedures.

6.2   Damping

Based on previous experience with the bridge, there was no realistic expectation to provide single reliable damping estimates for each mode, and the estimates provided in this paper are not to be regarded as definitive: They are presented in order to indicate performance of the techniques. This is in contrast to the mode shape and frequency estimates which are reliable enough to be used for structural identification purposes.

Damping values are known to vary with wind speeds (Cheli et al., 1992) and the various estimation methods are known to have associated errors which come in the form of variance and bias. These were both investigated in relation to the 1980s technology for OMA (Brownjohn, 1994).

The phenomenon of positively biased damping values was examined at length for the 1985 study as contributing, along with a variety of physical mechanisms, to values observed in system identification. In the 1985 study values were estimated by curve fitting to auto spectra and it was demonstrated that using longer records (with assumed stationarity) and hence finer frequency spacing led to convergence at more realistic damping values, with the study by BRE

(Littler, 1992) producing estimates as low as 1% for the fundamental vertical mode, although the more achievable lower bound is 2%, confirmed by applying both NExT/ERA and SSI-COV to a complete, but not too windy, day of deck vertical response.

Time domain techniques such as SSI-COV and ERA for damping estimation offer improved accuracy and there are procedures for estimating reliability of parameters for SSI (Reynders et al., 2008) but the fundamental limits do not disappear, leaving a significant problem for reliable damping estimation of tall, low damping structures in subject to time-varying environment and loads.

Nevertheless baseline values representing 'structural damping' in still air are needed if aero-elastic effects are to be identified from changes 'in wind', which is the common approach for section model wind tunnel testing. With improved system identification procedures now available, it might be possible to extend the real time OMA to real time automated aero-elastic parameter identification, interpreting the in-wind changes through aero-elastic derivatives representing stiffness and damping effects of wind-structure interaction. Analysis of the in-deck continuously monitored response using SSI-COV provides pointers for the best approach e.g. using an ensemble of estimates from relatively short periods having similar environmental parameters.

6.3 Comparison with 1985 data

Table 1 and Table 2 also compare 2008 frequency estimates with those obtained in 1985. The last column in each table presents the percentage difference between the average values from the 2008 values compared to the 1985 values. All the vertical modes found in the 1985 study (and a few more at higher frequencies) have been found, while a more comprehensive set of lateral modes was identified. In addition the corresponding mode shapes have been mapped out with greater resolution and reliability.

For the vertical/torsional modes the changes in natural frequency shown in the two tables are

small and similar to the standard deviation values obtained from the in-deck estimation (Table 3). Even so the changes are consistently negative, around 1%. For the lateral modes the differences are not consistent, and reflect the greater degree of uncertainty in these values.

7 Conclusions

Several operational modal analysis techniques have been evaluated against each other as part of an exercise to provide an updated and more comprehensive modal model of the Humber Bridge.

NExT/ERA, SSI-COV and p-LSCF were applied by two teams of researchers to post-process the same dataset, and the modal parameters were compared to provide the best estimates of mode shape and frequency for vertical, lateral, torsional modes up to 1Hz.

Of all the methods, SSI-COV performed the best, identifying practically all possible modes. SSI-COV is a popular procedure that now benefits from automated assessment of stability plots and algorithms for assessing parameter variance errors. Hence the parameter estimates obtained from SSI are being used for the model calibration.

A variant of SSI is now used for the continuous monitoring, benefitting from the experience with the in-deck monitoring.

8 Acknowledgements

9   References

References

Abdel-Ghaffar, A. M., Scanlan, R. H., (1985). Ambient vibration studies of Golden Gate bridge: 1. Suspended structure, and 2. Pier tower structure. ASCE Journal of Engineering Mechanics 111, No. 4, 463-499.

Andersen, J. E., Fustinoni, M., (2006). Structural Health Monitoring Systems. COWI-Futurtec, Lyngby, Denmark.

Ashkenazi, V., Roberts, G. W., (1997). Experimental monitoring of the Humber Bridge using GPS. ICE Proceedings Civil Engineering 120, 177-182.

Bathe, K.-J., Wilson, E. L., and Petersen, F. E., (1974). SAPIV a structural analysis program for static and dynamic response of linear structures. University of California Report No. EERC 73-11,

Brownjohn, J M W and Worden, K., (2008). Novel data mining and performance diagnosis systems for structural health monitoring of suspension bridges.
http://gow.epsrc.ac.uk/ViewGrant.aspx?GrantRef=EP/F035403/1

Brownjohn, J. M. W., Dumanoglu, A. A., Severn, R. T., (1992). Ambient vibration survey of the Fatih Sultan Mehmet (Second Bosporus) Suspension Bridge. Earthquake Engineering and Structural Dynamics 21, 907-924.

Brownjohn, J. M. W., (1990). Humber bridge monitoring: Digital measurements March-May 1990 and preliminary analysis. Report UBCE-EE-90-10 University of Bristol Department of Civil

Engineering,

Brownjohn, J. M. W., (1994). Estimation of damping in suspension bridges. Structures and Buildings, Proceedings, Institution of Civil Engineers 104, 401-415.

Brownjohn, J. M. W., Bocciolone, M., Curami, A., Falco, M., Zasso, A., (1994). Humber Bridge full scale measure campaigns 1990-1991. Wind Engineering and Industrial Aerodynamics 52, 185-218.

Brownjohn, J. M. W., Carden, E. P., (2007). Tracking the effects of changing environmental conditions on the modal parameters of Tamar Bridge. In: 3rd International Conference on Structural Health Monitoring and Intelligent Infrastructure, Vancouver, Canada.

Brownjohn, J. M. W., Dumanoglu, A. A., Severn, R. T., Blakeborough, A. B., (1989). Ambient vibration survey of the Bosporus suspension bridge. Earthquake Engineering and Structural Dynamics 18, 263-283.

Brownjohn, J. M. W., Dumanoglu, A. A., Severn, R. T., Taylor, C. A., (1987). Ambient vibration measurements of the Humber Suspension Bridge and comparison with calculated characteristics. Proceedings Institution of Civil Engineers Part 2 83, 561-600.

Brownjohn, J. M. W., Hao, H., and Pan, T.-C., (2001). Assessment of structural condition of bridges by dynamic measurements. Nanyang Technological University, Applied Research Project RG 5/97. Singapore

Brownjohn, J. M. W., Pavic, A., Carden, E.P., Middleton, C.J., (2007). Modal testing of Tamar suspension bridge. In: IMAC XXV, Orlando.

Carder, D. S., (1937). Observed vibrations of bridges. Bulletin Seismological Society of America 27, 267.

Cheli, F., Collina, A., Diana, G., Zasso, A., Brownjohn, J. M. W., (1992). Suspension bridge parameter identification in full-scale test. Journal of Wind Engineering and Industrial Aerodynamics 41, 165-176.

Cheung, M. S., Tadros, G. S., Brown, J., Dilger, W. H., Ghali, A., Lau, D. T., (1997). Field monitoring and research on performance of the Confederation Bridge. Canadian Journal of Civil Engineering 25, 951-962.

Conte, J. P., He, X., Moaveni, B., Masri, S. F., Caffrey, J. P., Wahbeh, M., Tasbihgoo, F., Whang, D. H., Elgamal, A., (2008). Dynamic Testing of Alfred Zampa Memorial Bridge. ASCE Journal of Structural Engineering 134, No. 6, 1006-1015.

Cunha, A., Caetano, E., Delgado, R., (2001). Dynamic tests on a large cable-stayed bridge. ASCE Journal of Bridge Engineering 6, No. 1, 54-62.

Cunha, A., Caetano, E., Magalhaes, F., (2007). Output-only dynamic testing of bridges and special structures. Structural Concrete 8, No. 2, 67-85.

Curami, A., Falco, M., Zasso, A., (1992). Nonlinear effects in sectional model aeroelastic parameters identification. pp. 1321-1332.

Diana, G., Falco, M., Cheli, F., Cigada, A., (2003). The aeroelastic study of the Messina Straits Bridge. pp. 79-106.

Dumanoglu, A. A., Brownjohn, J. M. W., Severn R.T., (1992). Seismic analysis of the Fatih Sultan

Mehmet (Second Bosporus) Suspension Bridge. Earthquake Engineering and Structural Dynamics 21, 881-906.

Dumanoglu, A. A. and Severn, R. T., (1985). Asynchronous seismic analysis of modern suspension bridges. Part 1: Free vibration. Research Report University of Bristol Department of Civil Engineering,

Dumanoglu, A. A., Severn, R. T., (1987). Seismic response of modern suspension bridges to asynchronous vertical ground motion. Proceedings ICE Part 2 83, 701-730.

Fitzpatrick, A., Dallard, P., le Bourva, S., Low, A., Ridsill Smith, R., and Willford, M., (2001). Linking London: The Millennium Bridge. The Royal Academy of Engineering, London

Frandsen, J. B., (2001). Simultaneous pressure and accelerations measured full-scale on the Great Belt East suspension bridge. Journal of Wind Engineering and Industrial Aerodynamics 89, No. 1, 95-129.

Gurney, T. J. R., (1983). Humber Bridge. Mining Technology Vol. 65 No. 758, 465-468.

Highways Dept, Hong Kong, (1993). WASHMS system specification.

Honshu-Shikoku Bridge Authority, (1987). Observation of Ohnaruto bridge behaviour. Honshu-Shikoku Bridge Authority Bridge and Offshore Engineering Association, Japan,

Hoult, N. A., Fidler, P. R. A., Wassell, I. J., Hill, P. G., Middleton, C. R., (2008). Wireless structural health monitoring at the Humber Bridge UK. ICE Proceedings Bridge Engineering 161, No. 4, 189-195.

James III, G. H., Carne, T. G., Lauffer, J P., (1995). The Natural Excitation Technique (NExT) for

Modal Parameter Extraction from Operating Structures. The International Journal of Analytical and Experimental Modal Analysis 10, No. 4, 260-277.

Juang, J.-N., Pappa, R. S., (1985). An eigensystem realization algorithm for modal parameter identification and model reduction. Journal of Guidance 8, No. 5, 620-627.

Koh, H.-M., PArk, W., Choo, J. F., (2009). Achievements and challenges in bridge health monitoring systems and intelligent infrastructures in Korea. In: 4th International Conference on Structural Health Monitoring of Intelligent Infrastructure (SHMII-4), Zurich. 1-14

Kumarasena, T., Scanlan, R. H., Morris, G. R., (1989). Deer Isle bridge: Field and computed vibrations. ASCE Journal of Structural Engineering no.9 VOL. 115, 2313-2328.

Larsen, A., Esdahl, S., Andersen, J. E., Vejrum, T., (2000). Storebaelt suspension bridge - vortex shedding excitation and mitigation by guide vanes. Journal of Wind Engineering and Industrial Aerodynamics 88, No. 2-3, 283-296.

Le Diourion, T., Hovhanessian, G., (2005). The health monitoring of Rion Antirion Bridge. In: IMACXXIII, Orlando.

Littler, J. D., (1992). Ambient vibration tests on long span suspension bridges. Journal of Wind Engineering and Industrial Aerodynamics 42, No. 1-3, 1359-1370.

Lo, W., Shih, C., Hinote, G., (2001). Ground vibration test of a commercial aircraft. In: IMACXIX, Orlando, FL.

Macdonald, J. H. G., Irwin, P. A., Fletcher, M. S., (2002). Vortex-induced vibrations of the Second Severn Crossing cable-stayed bridge -full-scale and wind tunnel measurements. ICE Proceedings

-Structures and Buildings 152, No. 2, 123-134.

Magalhaes, F., Cunha, A., Caetano, E., (2009a). Online automatic identification of the modal parameters of a long span arch bridge. Mechanical Systems and Signal Processing 23, No. 2, 316-329.

Magalhaes, F., Reynders, E., Cunha, A., De Roeck, G., (2009b). Online automatic identification of modal parameters of a bridge using the p-LSCF method. In: International Operational Modal Analysis Conference, Portonovo, AN, Italy.

Miyata, T., Yamada, H., Katsuchi, H., Kitigawa, M., (2002). Full-scale measurement of Akashi-Kaikyo bridge during typhoon. Journal of Wind Engineering and Industrial Aerodynamics 90, 1517-1527.

Nayeri, R. D., Tasbihgoo, F., Wahbeh, M., Caffrey, J. P., Masri, S. F., Conte, J. P., Elgamal, A., (2009). Study of time-domain techniques for modal parameter identification of a long suspension bridge with dense sensor arrays. ASCE Journal of Engineering Mechanics 135, No. 7, 669-683.

Nigbor, R. L., (1984). Full-scale ambient vibration measurements of the Golden Gate suspension bridge- instrumentation and data acquisition. In: 8WCEE Vol. 6,

Okauchi, I., Tanaka, A., Iwaya, K., Furuya, N., (1986). Vibration test of Ohnaruto Bridge to confirm windproofness. In: IABSE Symposium, Tokyo.

Pakzad, S. N., Fenves, G. L., (2009). Statistical Analysis of Vibration Modes of a Suspension Bridge Using Spatially Dense Wireless Sensor Network. Journal of Structural Engineering 135, No. 7, 836-872.

Pappa, R. S., Elliott, K. B., (1993). Consistent-Mode Indicator for the Eigensystem Realization-Algorithm. Journal of Guidance Control and Dynamics 16, No. 5, 852-858.

Pavic, A., Miskovic, Z., Zivanovic, S., (2008). Modal properties of beam-and-block pre-cast floors. The IES Journal Part A: Civil & Structural Engineering 1, No. 3, 171-185.

Peeters, B., van der Auweraer, H., Guillaume, P., Leuridan, J., (2004). The PolyMAX frequency-domain method: a new standard for modal parameter estimation? Journal of Shock and Vibration 11, No. 3-4, 395-409.

Reynders, E., Pintelon, R., De Roeck, G., (2008). Uncertainty bounds on modal parameters obtained from stochastic subspace identification. Mechanical Systems and Signal Processing 22, No. 4, 948-969.

Siringoringo, D. M., Fujino, Y., (2006). Observed dynamic performance of the Yokohame-Bay Bridge from system identification using seismic records. Structural Control and Health Monitoring 13, 226-244.

Stephen, G. A., Brownjohn, J. M. W., Taylor, C. A., (1993). Measurements of static and dynamic displacement from visual monitoring of the Humber Bridge. Engineering Structures 15, 197-208.

Structural Vibration Solutions, (2009). Stonecutters Bridge.
http://www.svibs.com/documentation/case_stonecutters_bridge.htm

Tezcan, S. S., Ipek, M., Petrovski, J., Paskalov, T., (1975). Forced vibration survey of Istanbul Bogazici bridge. In: 5th European Conference on Earthquake Engineering, Istanbul.

University of Washington, (1954). Aerodynamic stability of suspension bridges with special

reference to the Tacoma Narrows bridge. Bulletin No. 116 University of Washington Engineering Experiment Station,

Van Overschee, P., De Moor, B., (1996). Subspace Identification for Linear Systems. Kluwer Academic Publishers.

Vincent, G. S., (1962). Golden Gate bridge vibration studies. Transactions of the American Society of Civil Engineers 127, 667-707.

Wong, K. Y., (2004). Instrumentation and health monitoring of cable-supported bridges. Structural Control and Health Monitoring 11, No. 2, 91-124.

Xu, Y. L., Ko, J. M., Zhang, W. S., (1997). Vibration studies of Tsing Ma suspension bridge. ASCE Journal of Bridge Engineering 2, No. 4, 149-156.

Zasso, A., Vergani, M., Bocciolione, M., Evans, R., (1993). Use of a newly designed optometric instrument for long term, long distance monitoring of structures, with an example of its application on the Humber bridge. In: Second International Conference on Bridge Management, Guildford.

Table 1 Comparison of the results delivered by the NExT/ERA, SSI-COV and p-LSCF methods with the 1985 results for vertical and torsional (highlighted) modes. Mode number (#) corresponds to Figure 9.

type	#	symmetry	ERA		SSI-COV		p-LSCF		UoB (1985)		%change
			Hz	%	Hz	%	Hz	%	Hz	%	
V	1	Ss, Ms, Ls-S	0.116	3.4	0.116	3.1	0.116	3.3	0.117	3.9	-0.6
V	2	Ss, Ls-S; Ms-A	0.153	8.9	0.149	8.1	0.153	6.6	0.154	4.0	-1.3
V	3	Ss, Ms, Ls-S	0.175	7.1	0.172	4.4	-	-	0.177	3.6	-2.1
V	4	Ss, Ms, Ls-S	0.215	3.5	0.215	2.7	0.215	2.2	0.218	3.1	-1.4
V	5	Ms-A; Ls-S	0.239	1.6	0.24	1.6	0.239	1.2	0.240	2.1	-0.1
V	6	Ms-S	0.308	1.2	0.309	1.3	0.311	1.1	0.310	1.8	-0.2
T	**7**	**MS, Ls-S**	**0.309**	**1.3**	**0.308**	**0.9**	**0.308**	**1.0**	**0.311**	1.5	-0.9
V	8	Ms-A; Ls-S	0.381	1.5	0.381	1.4	0.38	1.2	0.383	1.2	-0.6
V	9	Ms-S	0.462	1.1	0.462	0.9	0.462	1.0	0.464	1.1	-0.4
T	**10**	**Ms-A; Ls-S**	**0.479**	**0.8**	**0.479**	**0.7**	**0.477**	**0.7**	**0.482**	1.2	-0.7
V	11	Ms-A; Ls-S	0.539	1.1	0.537	1.0	0.557	0.9	0.540	1.1	0.7
V	12	Ms-S	0.625	0.9	0.625	0.7	0.625	0.8	0.627	1.0	-0.4
T	**13**	**Ms-S**	**0.646**	**0.7**	**0.643**	**0.5**	**0.645**	**0.6**	**0.650**	1.0	-0.8
V	14	MS-A	0.717	0.9	0.716	0.9	0.716	0.8	0.720	0.9	-0.5
V	15	Ms-S	0.810	0.8	0.809	0.7	0.809	0.6	0.814	0.9	-0.6
T	**16**	**Ms-A**	**0.851**	**0.9**	**0.848**	**0.8**	**0.849**	**0.6**	**0.858**	0.9	-1.0
V	17	Ms-S	0.910	0.9	0.909	0.7	0.908	0.69	0.913	0.8	-0.4

Key:　　　Ms=strong mode in main span

Ls=strong mode in long (Hessle) side span

Ss=strong mode in short (Barton) side span

-A is mode with odd number of nodes

-S is mode with even number of nodes

V is mode with dominant vertical motion

T is mode with dominant torsional motion

UoB (1985) University of Bristol results (Brownjohn et al., 1987)

Table 2 Comparison of the results delivered by the NExT/ERA, SSI-COV and p-LSCF methods with the 1985 results for lateral modes. Mode number (#) corresponds to Figure 10.

#	Symmetry	ERA		SSI-COV		p-LSCF		UoB (1985)		%change
		Hz	%	Hz	%	Hz	%	Hz	%	
1	Ms-S	0.056	8.3	0.056	6.0	0.055	4.0	0.056	9.3	-0.6
2	Ms-A	0.141	17.0	0.130	9.3	0.134	7.4	0.143	4.5	-5.6
3	Ms-S, Ls-S	0.246	1.3	0.236	5.0	0.238	2.7	0.239	4.2	0.4
4	Ms-A	-	-	0.378	1.4					
5	Ms-S	0.401	1.0	0.401	0.6	0.404	0.2	0.400	1.0	0.5
6	Ms-A; Ls-S	0.464	3.9	0.442	2.6	0.455	4.3	0.465	1.3	-2.4
7	Ms-S, Ls-A	0.518	2.4	0.510	0.9	0.508	2.5	0.510	1.0	0.4
8	(Ms-S)	-		0.550	0.4					
9	Ms-S	-		0.582	0.6					
10	Ms-S;Ss-S,Ls-A	0.632	6.4	0.640	1.8	0.625	1.8			
11	Ms-A	0.869	5.2	-						

Key: Ms=strong mode in main span

Ls=strong mode in long (Hessle) side span

Ss=strong mode in short (Barton) side span

-A is mode with odd number of nodes

-S is mode with even number of nodes

UoB refers to 1985 University of Bristol results (Brownjohn et al., 1987)

Table 3 Frequency and damping estimates using SSI-COV for in-deck monitor for different averaging periods. Standard deviation values (σ) express variation over all estimates rather than overall parameter reliability.

Vertical	$\mu(f)$/Hz			$\sigma(f)$/Hz			$\mu(\zeta)$/%			$\sigma(\zeta)$/%		
	20m	60m	120m	20m	60m	120m	20m	60m	120m	20m	60m	120m
mode 1	0.1163	0.1164	0.1163	0.0017	0.0014	0.0013	1.47	1.85	2.15	0.6	0.65	0.8
mode 5	0.2398	0.2399	0.2399	0.0016	0.0013	0.0008	0.72	0.83	0.96	0.24	0.27	0.15
mode 6	0.3103	0.3101	0.3101	0.0018	0.0017	0.0016	0.42	0.63	0.78	0.1	0.1	0.11
Lateral	$\mu(f)$/Hz			$\sigma(f)$/Hz			$\mu(\zeta)$/%			$\sigma(\zeta)$/%		
	20m	60m	120m	20m	60m	120m	20m	60m	120m	20m	60m	120m
mode 2	0.1417	0.1411	0.1402	0.0106	0.01	0.011	1.62	2.63	4.56	1.04	1.4	1.84
mode 3	0.2403	0.2405	0.2405	0.0009	0.0005	0.0004	0.7	0.77	1.18	0.31	0.35	0.06
mode 4	0.3791	0.3794	0.3797	0.0046	0.0044	0.004	0.61	0.92	1.21	0.39	0.44	0.41
mode 5	0.4011	0.4014	0.4018	0.0015	0.0016	0.0015	0.37	0.37	0.41	0.2	0.15	0.13

Figure 1 View of Humber Bridge from West, Hessle side
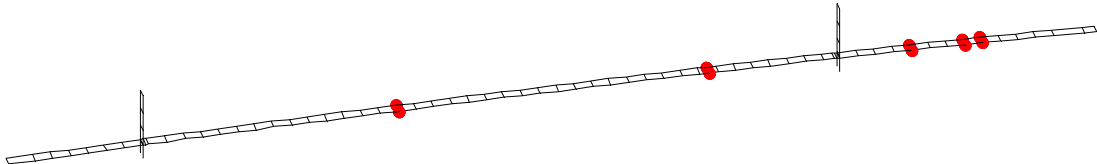
Figure 2 Sensor locations for setup24, which focuses on the Barton side span measurement.

h21 is the left most location
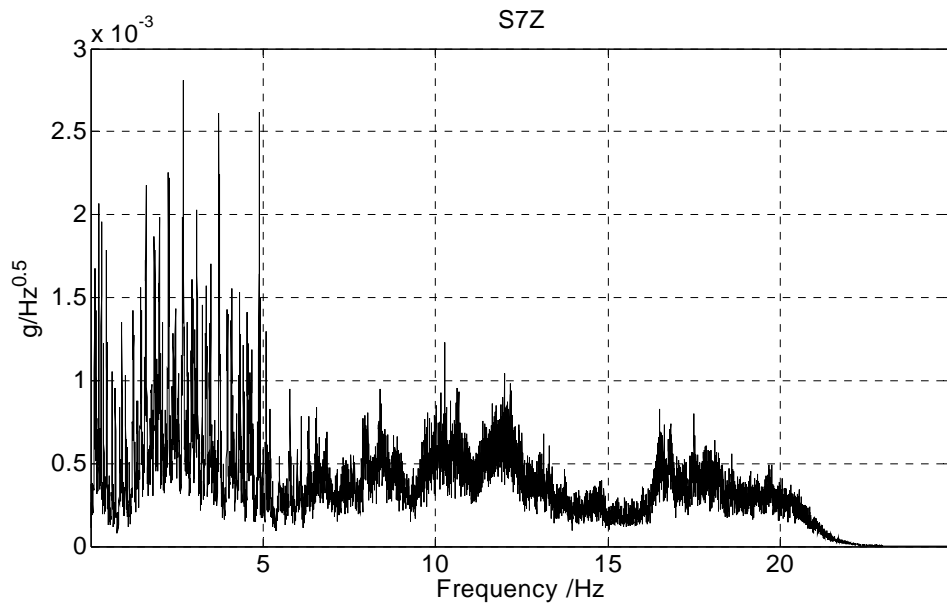
Figure 3 Vertical auto spectra at h21
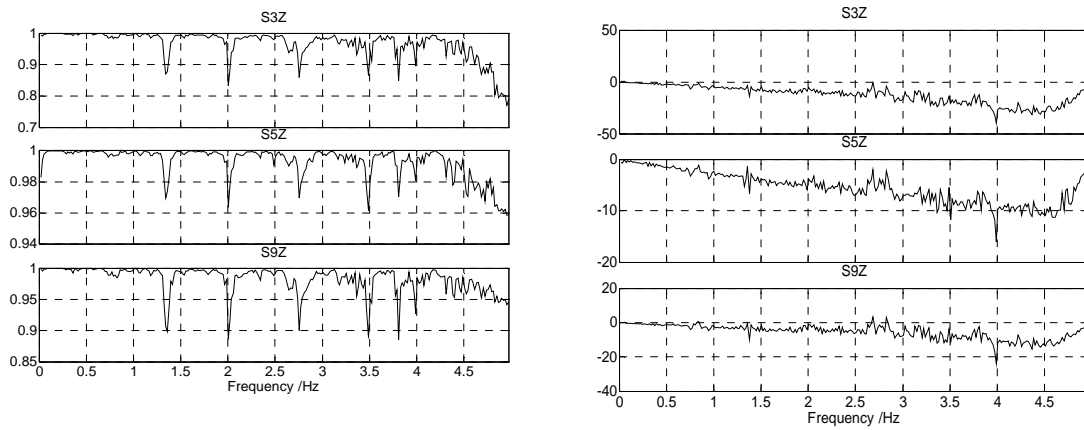
Figure 4 Coherence functions (left) and phase angles (right) with respect to reference channel in

sensor S1
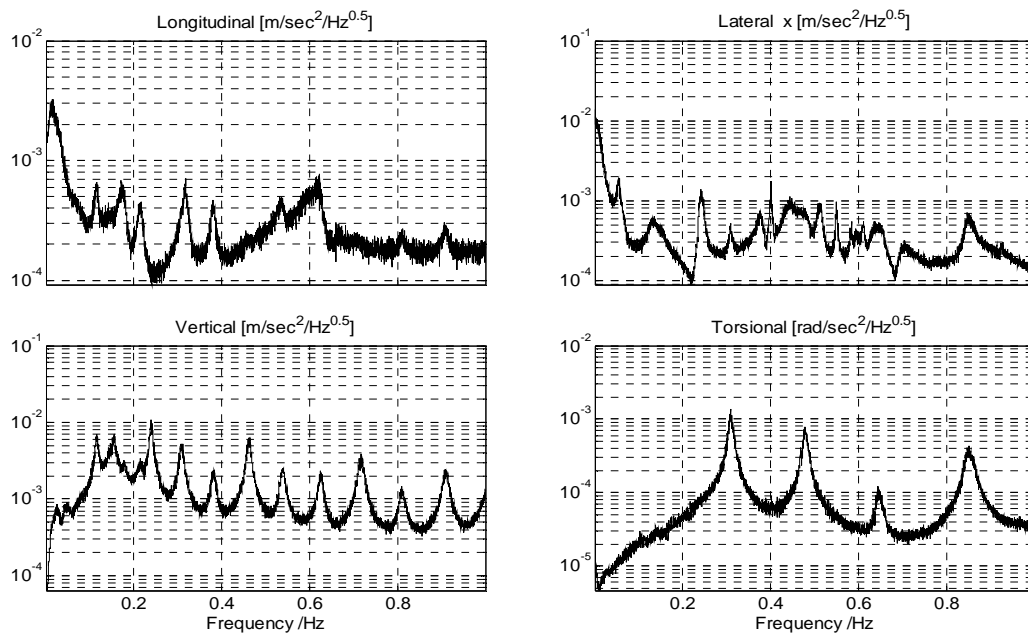
Figure 5 Auto spectra of significant degrees of freedom at h21in range 0-1Hz
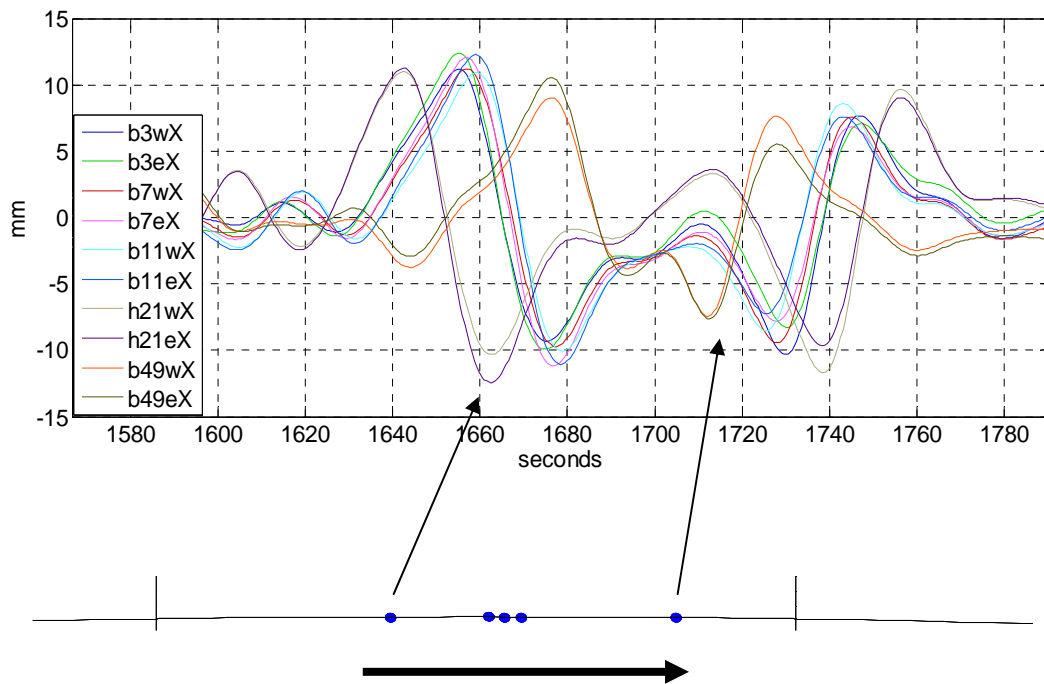
Figure 6 Quasi-static relative vertical displacements across box girder induced by passing

vehicle, obtained from DC component of lateral acceleration signals. b,h refer to

Barton (left) and Hessle (right) side of midspan, X is lateral direction.

Half-sum of the deck vertical accelerations
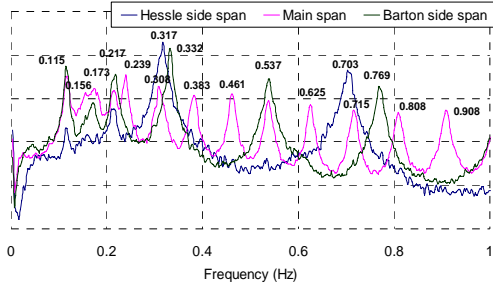
Half-difference of the deck vertical accelerations
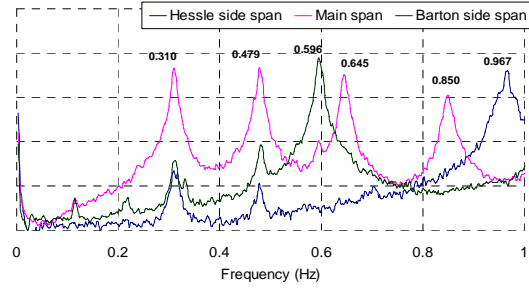
Half-sum of the deck lateral accelerations
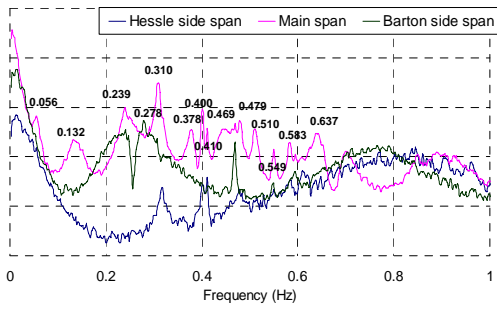
Towers accelerations
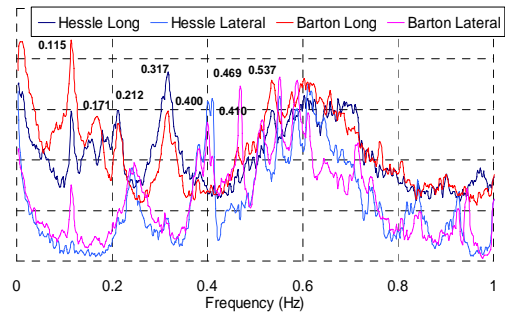
Figure 7 Average normalized power spectral densities (ANPSD) .
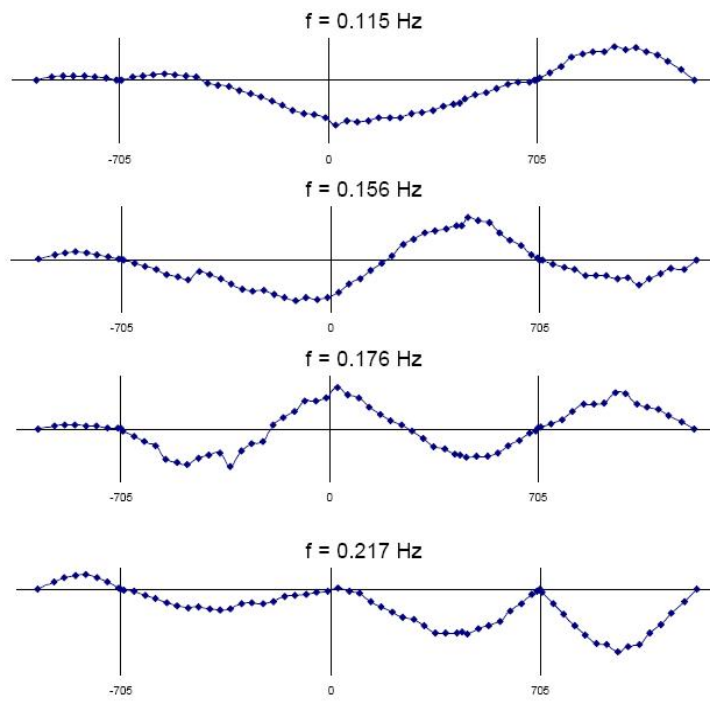
Figure 8 Some mode shapes identified with the Peak-Picking method
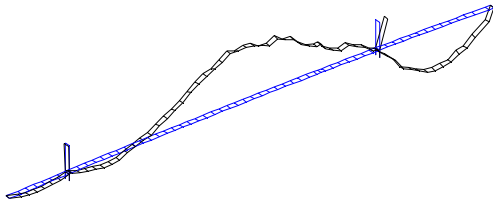
Mode 1: f=0.117Hz ζ=3.9%
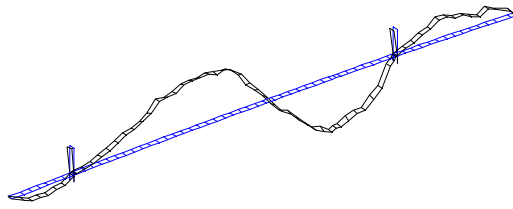
Mode 2: f=0.154Hz ζ=4%
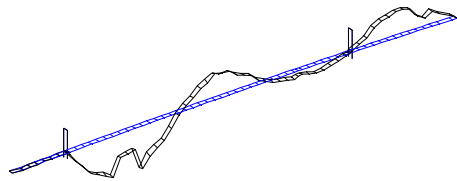
Mode 3: f=0.177Hz ζ=3.6% (No tower DOFs)
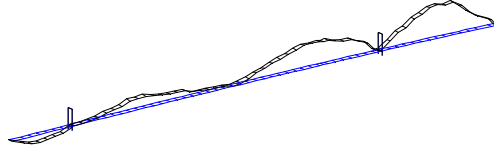
Mode 4: f=0.218Hz ζ=3.1% (No tower DOFs)
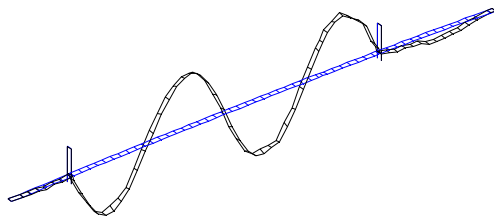
Mode 5: f=240Hz ζ=2.1%
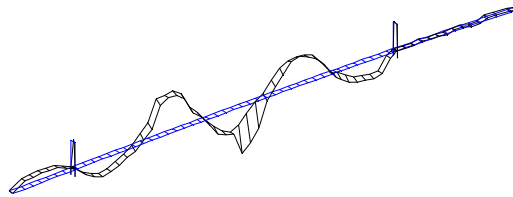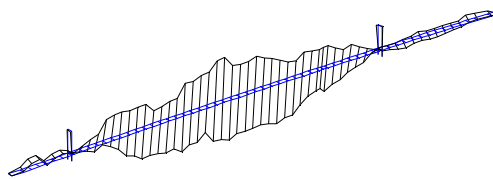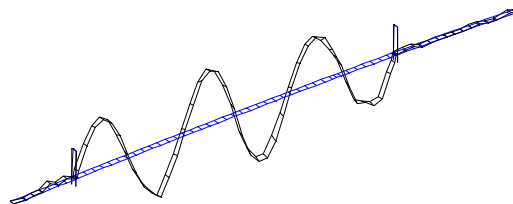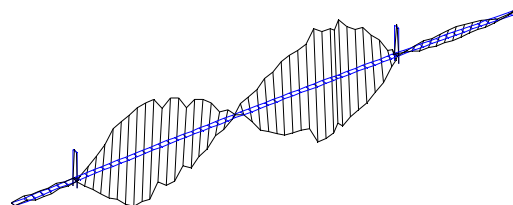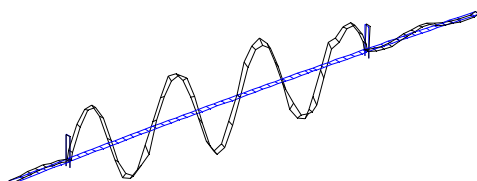
Mode 6: f=0.310Hz ζ=1.8%

Mode 7: f=0.311Hz ζ=1.5%

Mode 8: f=0.383Hz ζ=1.2%

Mode 9: f=0.464Hz ζ=1.1%   Mode 10: f=0.482Hz ζ=1.2%
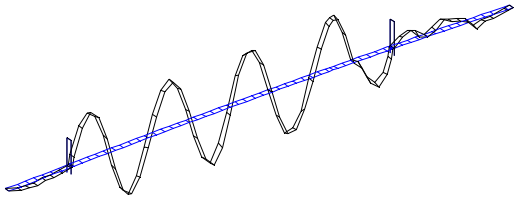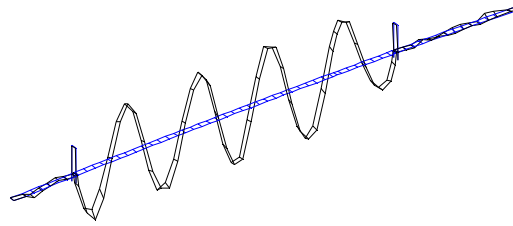
Mode 11: f=0.540Hz ζ=1.1%   Mode 12: f=0.627Hz ζ=1.0%
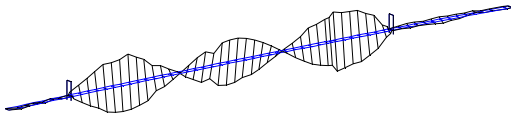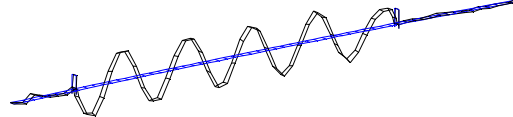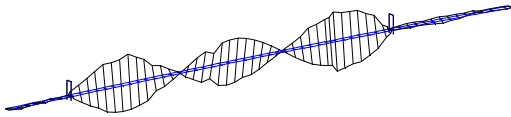
Mode 13: f=0.650Hz ζ=1.0% (No tower DOFs)   Mode 14: f=0.720Hz ζ=0.9%
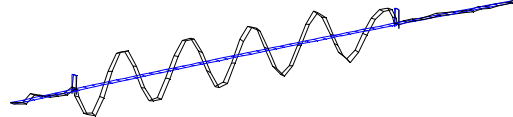
Figure 9 Modes identified using NExT/ERA applied to all vertical response DOFs
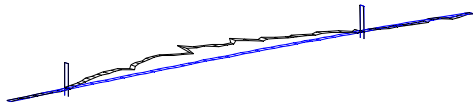
Mode 1: f=0.056Hz ζ=8.3%

Mode 2: f=0.141Hz ζ=17%

Mode 3: f=0.246Hz ζ=1.3%

f=0.309Hz ζ=1.2%
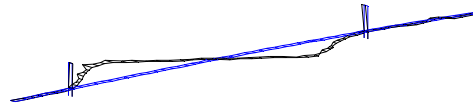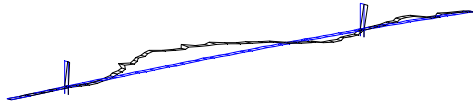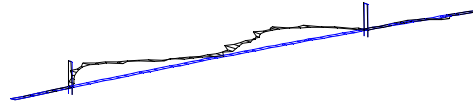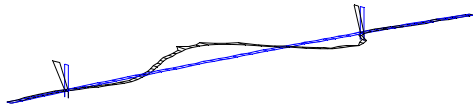
Mode 5: f=0.401Hz ζ=0.98%

Mode 6a: f=0.418Hz ζ=4.0%

Mode 6b: f=0.464Hz ζ=3.9%

f=0.484Hz ζ=1.2%
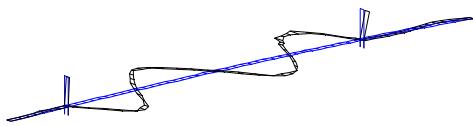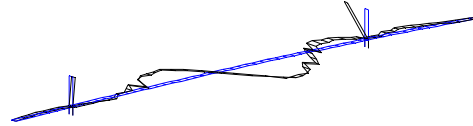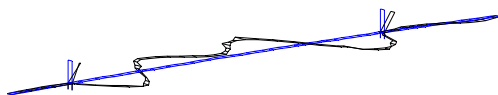
Mode 7: f=0.518Hz ζ=2.4%
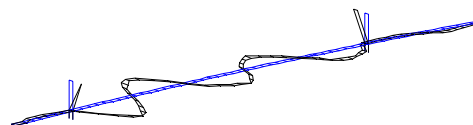
Mode 10: f=0.632Hz ζ=6.4%

Figure 10 Lateral deck and tower modes from NExT/ERA
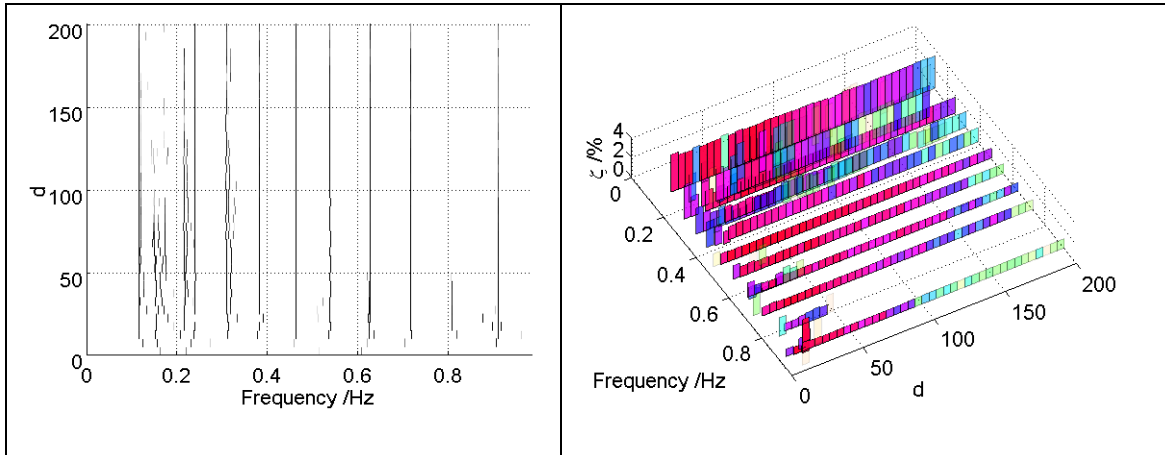
Figure 11 Stability of ERA frequency (left) and damping (right) estimates for 40 poles and up to

d=200 lags. Light/blue shades in damping plot indicate low EMAC values.
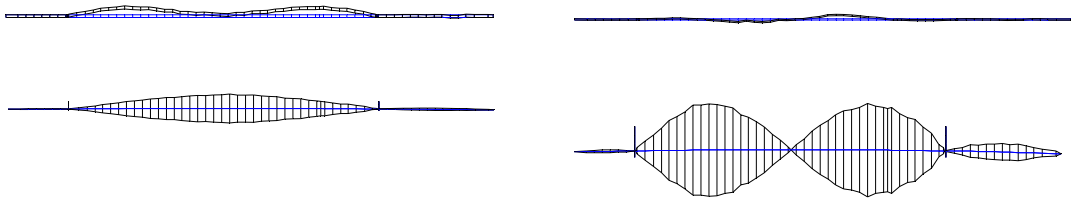
Mode T1 f=0.311Hz ζ=1.5%   Mode T2 f=0..482Hz ζ=1.2%

Figure 12 Torsional mode shapes in plan and elevation to same scale
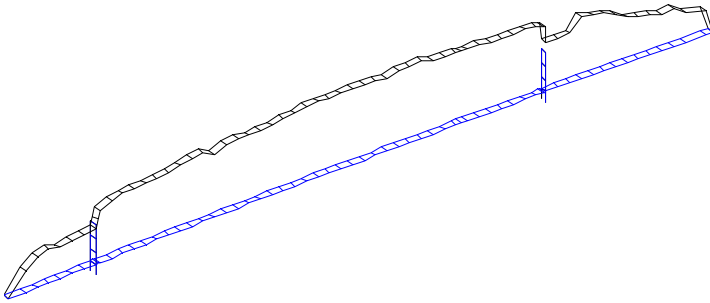
Mode Long1: f=0.615Hz ζ=2.5%

Figure 13 Longitudinal mode visualised as vertical movement of longitudinal degrees of

freedom

Half-sum of the deck vertical accelerations
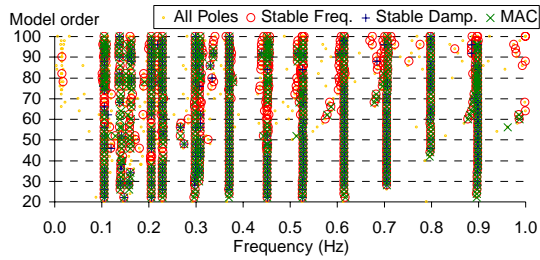
Half-difference of the deck vertical accelerations
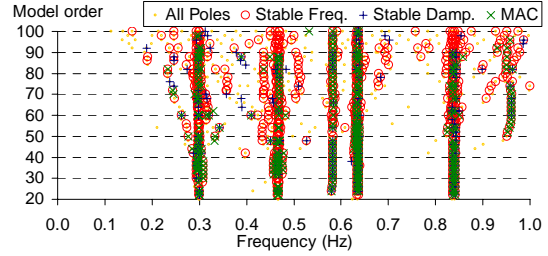
Half-sum of the deck lateral accelerations
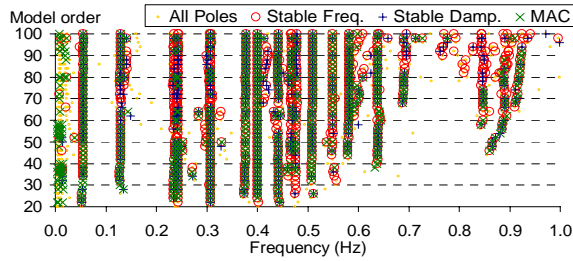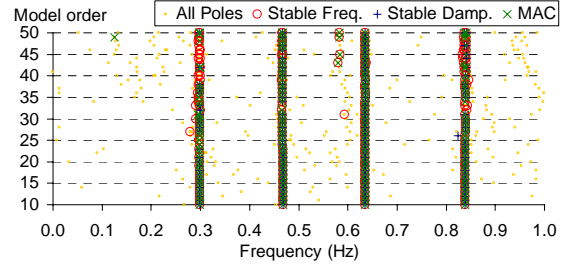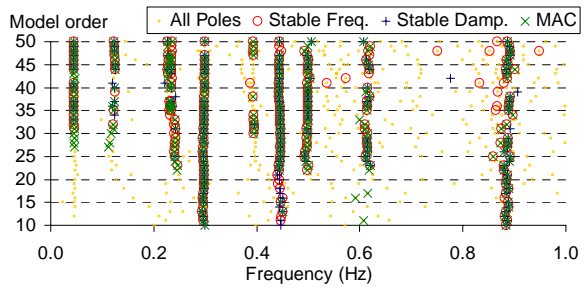
Figure 14 Stabilization diagrams produced by the SSI-COV method

$f_1 = 0.308\text{Hz} ; \xi = 0.94\%$

$f_3 = 0.643\text{Hz} ; \xi = 0.48\%$

$f_2 = 0.479\text{Hz} ; \xi = 0.65\%$

$f_4 = 0.848\text{Hz} ; \xi = 0.79\%$
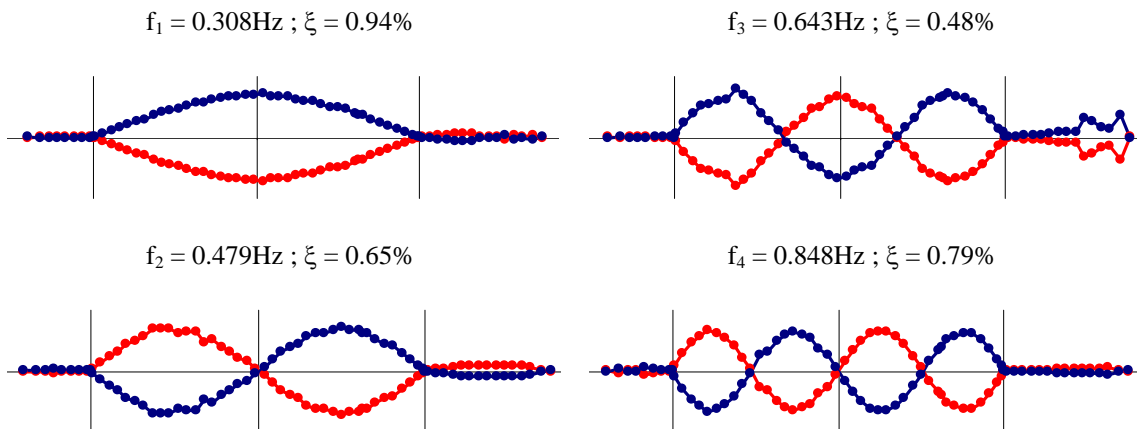
Figure 15 Torsion modes identified with the SSI-COV method
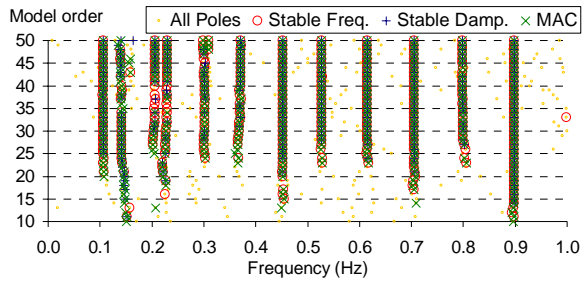
54

Half-sum of the deck vertical accelerations
Half-difference of the deck vertical accelerations

Half-sum of the deck lateral accelerations

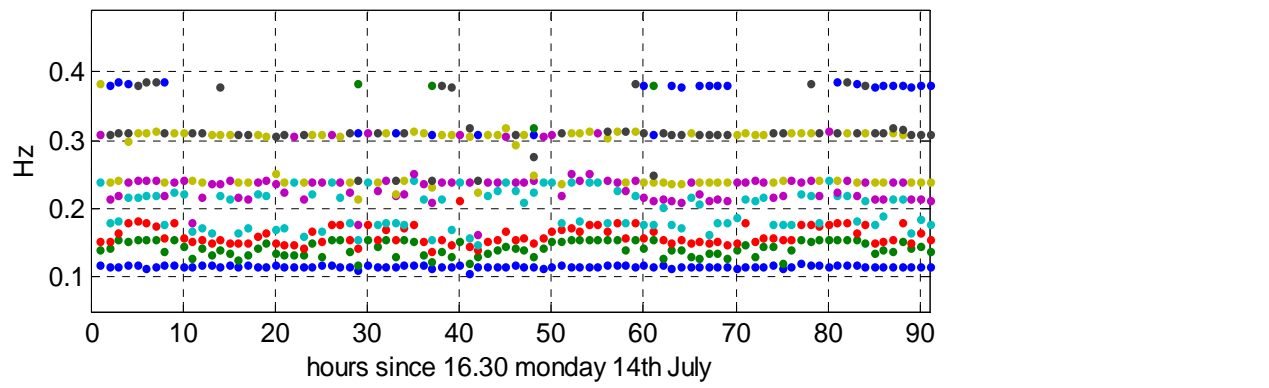Figure 16 Stabilization diagrams produced by the p-LSCF method

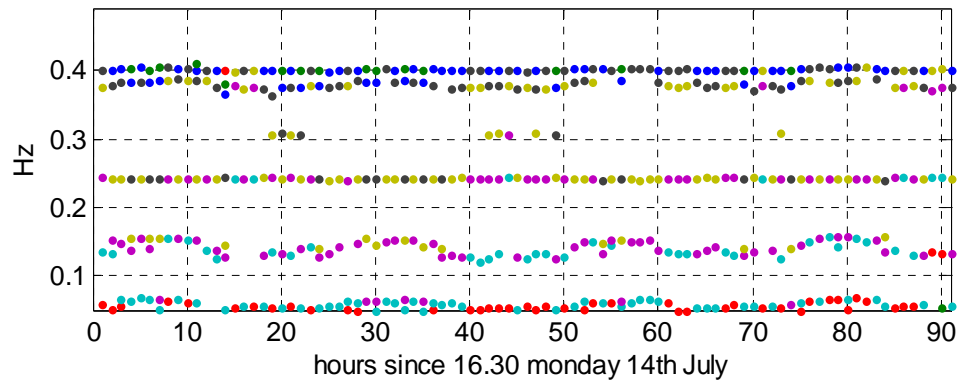Figure 17 Variation of vertical mode frequencies during testing.
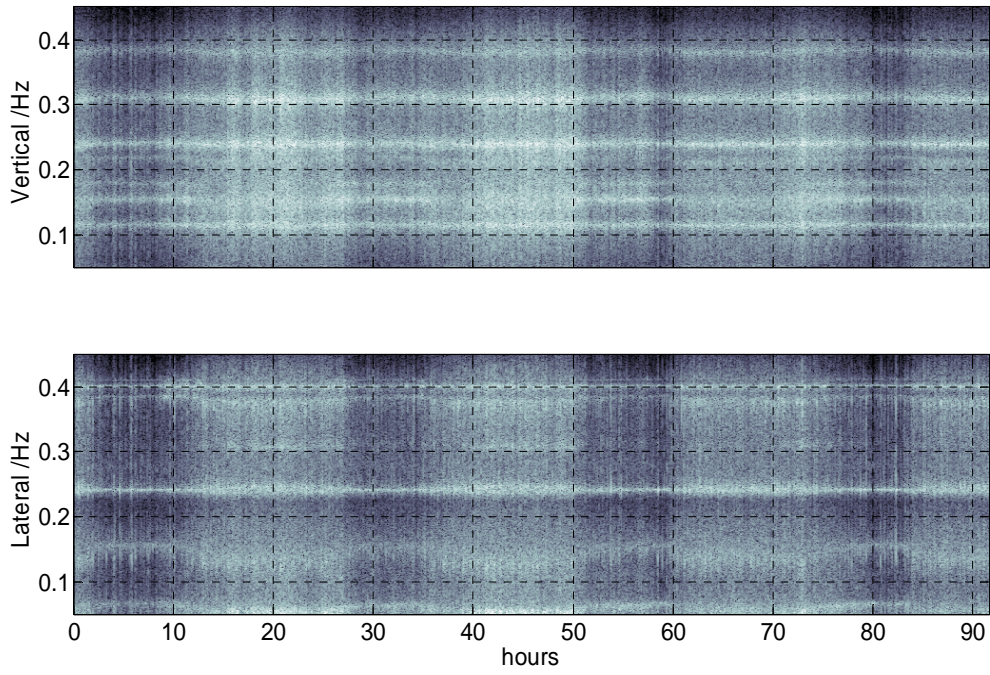

Figure 18 Variation of lateral mode frequencies during testing

Figure 19 Spectrogram of deck monitor acceleration response